# Use of Purified and Modified Bentonites in Linear Low-Density Polyethylene/Organoclay/Compatibilizer Nanocomposites

**Tijen Seyidoglu, Ulku Yilmazer**

*Department of Chemical Engineering, Middle East Technical University, Ankara 06531, Turkey*

Received 19 January 2011; accepted 7 May 2011
DOI 10.1002/app.34852
Published online 28 October 2011 in Wiley Online Library (wileyonlinelibrary.com).

**ABSTRACT:** Polyethylene-based ternary nanocomposites were prepared with different clay structures, obtained by the modification of purified Resadiye bentonite as the reinforcement, a random terpolymer of ethylene, butyl acrylate, and maleic anhydride with the trade name Lotader3210 as the compatibilizer, and linear low-density polyethylene (LLDPE) as the polymer matrix in an intensive batch mixer. The quaternary ammonium/phosphonium salts used for the modification of bentonite were dimethyldioctadecyl ammonium (DMDA) chloride (Cl), tetrakisdecyl ammonium (TKA) bromide (Br), and tributylhexadecyl phosphonium (TBHP) Br. The effects of the physical properties and structure of the organoclay on the clay dispersion were studied at different clay contents (2 and 5 wt %) and at a compatibilizer/organoclay ratio of 2.5. The extent of organoclay dispersion was determined by X-ray diffraction (XRD) and was verified by transmission electron microscopy (TEM), mechanical testing, and rheological analysis. XRD analysis showed that the nanocomposite with the organoclay DMDA contained intercalated silicate layers, as also verified by TEM. The TEM analysis of the nanocomposites with TBHP exhibited intercalated/partially exfoliated clay dispersion. TKA, with a crowded alkyl environment, sheltered and hindered the intercalation of polymer chains through the silicate layers. In comparison to pure LLDPE, nanocomposites with a 33–41% higher Young's modulus, 16–9% higher tensile strength, and 75–144% higher elongation at break were produced with DMDA and TBHP, respectively (at 5 wt % organoclay). The storage modulus increased by 807–1393%, and the dynamic viscosity increased by 196–339% with respect to pure LLDPE at low frequencies for the samples with DMDA and TBHP (at 5 wt % organoclay).
 J Appl Polym Sci 124: 2430–2440, 2012

**Key words:** compounding; nanocomposites; organoclay; polyethylene (PE); polymer rheology

## INTRODUCTION

Clay nanocomposites are a class of nanocomposites created by the dispersion of a refined form of nanoclay into polymer resins. Polymer–clay nanocomposites (PCNs) were first developed by Toyota in 1990 to produce timing belt covers.[1] Later, other automotive applications for nanocomposites were developed, such as a clay/nylon 6 nanocomposite covers for Mitsubishi engines and a clay/polyolefin nanocomposite step assistant for GM vehicles. Presently, PCNs have attracted researchers because of the remarkable improvement in product properties compared to those of pure polymers through the addition of a small amount of organoclay (2–5 wt %). Improvements include increases in the mechanical properties, that is, a higher modulus, an increase in strength,[2–7] an increase in the thermal properties,[8] a decrease in the permeability,[9,10] and reduced flammability.[8,11] The extent of these improved polymer properties is mainly dependent on the interfacial interactions between the polymer and the modified clay.

The initial structure of the montmorillonite contains several stacked layers with lateral dimensions of 100–200 nm, a layer thickness of approximately 1 nm, and an interlayer spacing (*d*-spacing) of approximately 1 nm. If these stacked layers are then separated into individual clay platelets, they would have individual aspect ratios on the order of 100–200. Such layers can substantially increase several properties of the polymer, at particularly low loading levels, because of the high aspect ratio of the reinforcement. Several factors can affect the properties of PCNs, including the concentration of clay used as a reinforcement, the effects of polymer immobilization by adsorption on clay surfaces, weak crosslinking due to bridging molecules

*Correspondence to:* U. Yilmazer (yilmazer@metu.edu.tr).
Contract grant sponsor: Scientific and Technical Research Council of Turkey, TUBITAK (through International Research Scholarship Programme-2214 to T.S.).
Contract grant sponsor: Middle East Technical University; contract grant number: BAP-2006-07-02-00-01.

between clay tactoids, and the alternation in the crystallinity of the polymer.[12]

The process of dispersing clay layers into the polymer matrix is strongly dependent on the polymer–clay compatibility. It is difficult to separate the individual clay platelets in nonpolar polymers such as polyolefins because of the natural polarity and hydrophilicity of the clay. To achieve this separation, the clay should be made more organophilic by pretreatment with amino acids, quaternary long alkyl length ammonium/phosphonium salts, tetra organic phosphonium solution, and ionic liquids.[13–16] However, even in the modified form, organoclays cannot easily be dispersed in nonpolar polyolefins without the help of a compatibilizer, which increases the interfacial interactions between the clay layers and polymer matrix. Compatibilizers have functional groups in their backbone that provide sufficient polarity to interact with silicate surfaces and aid in the dispersion of the polymer matrix. Maleic anhydride (MA) grafted polyolefins, mainly, polypropylene (PP) and polyethylene (PE), are the most widely used compatibilizers.[2,7,17,18]

The processing of polymer nanocomposites necessitates knowledge of their rheology. Because the rheological properties of particulate suspensions are responsive to the feature of the dispersed phase, they provide information about the internal microstructure of nanocomposites, such as the state of dispersion of clay and the confinement effect of silicate layers on the motion of polymer chains.[19,20] Consequently it can be used as a supplementary tool for other characterization techniques, such as X-ray diffraction (XRD), transmission electron microscopy (TEM), and mechanical testing. Superior to these traditional methods, the rheological properties are measured in the melt state, but this method examines the hybrid structure only indirectly.[21] Rheological characterization of PCNs has been carried out by many researchers to assess the degree of dispersion of clay layers.[7,19,22–25] In addition to the melt-mixing method that was used here, there exist novel *in situ* methods of preparing PE nanocomposites that result in highly improved properties.[26–28]

The aim of this study was to characterize and construct a connection between XRD and other characterization techniques, such as TEM, rheology, and mechanical characterization, to assess the degree of dispersion and the effect of clay structure on the final properties of the linear low-density polyethylene (LLDPE) matrix. Three organoclays with different alkyl chain lengths and structures were used. The quaternary ammonium/phosphonium salts used for the modification of purified bentonite (PB) were dimethyldioctadecyl ammonium (DMDA) chloride (Cl), tetrakisdecyl ammonium (TKA) bromide (Br), and tributylhexadecyl phosphonium (TBHP) Br. The organoclays modified with DMDA and TKA clay have not been used previously in the preparation of nanocomposites with LLDPE matrices. Stoeffler et al.[7] used organoclay modified by TBHP in a LLDPE matrix and characterized the nanocomposites by XRD, TEM, rheology, differential scanning calorimetry, and thermogravimetric analysis but not by mechanical testing.

**TABLE I**
**ICP Results for RB, PB, and DMDA**

| Component | RB (wt %) | PB (wt %) | DMDA (wt %) |
|---|---|---|---|
| MgO | 1.85 | 2.15 | 1.51 |
| CaO | 2.60 | 0.33 | 0.10 |
| $Fe_2O_3$ | 3.21 | 3.91 | 2.70 |
| $Al_2O_3$ | 15.6 | 16.83 | 11.8 |
| $Na_2O$ | 2.69 | 2.18 | 0.04 |
| $K_2O$ | 0.78 | 0.28 | 0.13 |
| $SiO_2$ | 54.97 | 61.1 | 41.88 |

## EXPERIMENTAL

### Materials

Raw bentonite (RB) was kindly provided by Karakaya Bentonit A. S. (Ankara, Turkey). Its chemical analysis, given in Table I, as determined by an inductively coupled plasma (ICP) optical emission spectrometer (PerkinElmer Inc., DRC II Model, MA, USA) showed high levels of $SiO_2$ and MgO; this indicated a high amount of montmorillonite. The organoclays used in this study were prepared by purification followed by modification of the mentioned salts.[29] The cation-exchange capacities of the RB and PB were determined by the methylene blue method to be 67.5 and 100 mmol/100 g of clay, respectively. PBs were modified with two quaternary alkyl ammonium salts, DMDA Cl and TKA Br, and one quaternary phosphonium salt, TBHP Br. The structures of the modifiers are shown in Table II. The abbreviations for the modified bentonites in Table II are based on the cation of the surfactant, for example, the term DMDA is used for the organoclay that was modified with DMDA Cl.

The LLDPE used as a polymer matrix was a product of Exxon Mobil, Corp., NY, USA (LL-1001 blown film resin, previous trade name MMA-042) and had a melt index of 1 g/10 min (ASTM D 1238, 190°C, 2.16 kg) and a density of 0.918 g/cm$^3$ (ASTM 1505). The commercial elastomeric material, a terpolymer of ethylene, butyl acrylate, and MA, with the trade name Lotader3210 (LOT), was obtained from Arkema, Inc., PA, USA. It had a reported melt index of 5 g/10 min and a density of 0.94 g/cm$^3$. Its butyl acrylate and MA contents were 6 and 3%, respectively.

### Preparation of the nanocomposites

LLDPE, LOT, and the organoclays were dried in an oven at 80°C for 12–15 h before compounding.

**TABLE II**
**Structures of the Modifiers**

| Modifier | Chemical structure of the surfactants | Abbreviation | *d*-spacing (Å) |
|---|---|---|---|
| None | — | PB | 12.0 |
| TKA $Br^-$ | 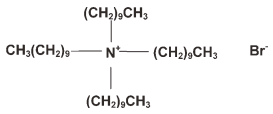 | TKA | 27.1 |
| DMDA $Cl^-$ | 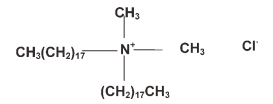 | DMDA | 26.4 |
| TBHP $Br^-$ | 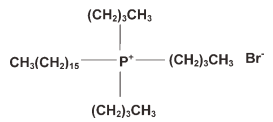 | TBHP | 22.4 |

The LLDPE-based ternary nanocomposites were prepared by melt mixing in a Haake mixer (Buchler Instruments, Inc., Saddle Brooke, NJ) with a mixing volume capacity of 300 mL, at 190°C and 32 rpm for 15 min. Nanocomposites with two different organoclay contents, 2 and 5%, were prepared at a LOT/organoclay ratio of 2.5. The nanocomposites are abbreviated as LLDPE/organoclay/LOT, in which the concentration of the organoclay and LOT are given at the end. LLDPE and LOT were fed to the mixer first, followed by the addition of organoclays. Binary composites of 98% LOT and 2% organoclay were prepared to observe the compatibility between the compatibilizer and the organoclays. These samples were abbreviated as LOT98/organoclay2. Neat LLDPE, LOT, and binary mixtures of LLDPE/LOT were melt-mixed so that they could undergo the same processing history as the ternary nanocomposites did. Abbreviations and concentrations of nanocomposites are given in Table III.

## XRD

The samples for X-ray analysis were prepared with a Carver Inc., IN, USA compression-molding instrument. Samples were compression-molded between two Teflon sheets in square-shaped molds. The temperature was kept between 190 and 200°C during compression molding. Materials were heated for 5 min for melting and then pressed at 4 bars for 1 min. The molds were cooled slowly with a tap-water circulation system for 8 min under pressure. Then, the pressure was released, and the materials were taken out.

XRD patterns were obtained with a Rigaku Miniflex diffractometer equipped with a Cu Kα source (1.5406 Å) operating at 30 kV and 15 mA. The diffraction patterns were collected in the Bragg angle (2θ) range of 2–5° at a scanning rate of 0.1° min and with a step size of 0.01°. The *d*-spacing was calculated from Bragg's law:

$$n\lambda = 2d \sin\theta$$

where $n$ is the degree of diffraction, λ is the wavelength, θ is the measured diffraction angle, and $d$ refers to the interlayer spacing.

## Mechanical properties

The samples for mechanical testing were prepared with a laboratory-scale DSM Xplore, Geleen, Netherlands (micro 10 cc) injection-molding machine. The injection pressure was 10 bars, and the melt and mold temperatures were 200 and 30°C, respectively. The hold time was 3.5 min for each sample.

The tensile properties were measured with a Shimadzu AG-IS machine with dog-bone-type molded samples. The samples had a gauge length of 30 mm, a thickness of 2.1 mm, and a width of 4 mm. Young's modulus was determined as the tangent of the initial elastic region. The gauge length, crosshead speed, and strain rate were 30 mm, 15 mm/min, and 0.5 $min^{-1}$, respectively. At least five samples were used for one set, and their averages are shown with standard deviation bars.

## TEM analysis

Morphology, that is, dispersion of clay layers were analyzed by TEM. Ultrathin sections approximately 70 nm thick were cryogenically cut with a diamond knife at a temperature of 100°C. All samples were trimmed parallel to the molding direction. A TEM instrument with a brand name of Tecnai™ G2 F30 produced by FEI Co., Oregon, USA with an accelerating voltage of 300 kV was used.

## Rheological characterization

The samples for rheological characterization were prepared with disk-shaped molds with a diameter of

**TABLE III**
**Abbreviations and Concentrations of the Composites**

| Composition | LLDPE | LOT | Organoclay |
|---|---|---|---|
| LLDPE | 100 | | |
| LOT | | 100 | |
| LLDPE95/LOT5 | 95 | 5 | |
| LLDPE87.5/LOT12.5 | 87.5 | 12.5 | |
| LOT98/DMDA2 | | 98 | 2 |
| LOT98/TBHP2 | | 98 | 2 |
| LOT98/TKA2 | | 98 | 2 |
| LLDPE/DMDA2/LOT5 | 93 | 5 | 2 |
| LLDPE/DMDA5/LOT12.5 | 82.5 | 12.5 | 5 |
| LLDPE/TBHP2/LOT5 | 93 | 5 | 2 |
| LLDPE/TBHP5/LOT12.5 | 82.5 | 12.5 | 5 |

25 mm and a thickness of 2 mm with the same conditions used in the preparation of compression-molded X-ray samples.

The samples were analyzed by a dynamic oscillatory rheometer in the melt state as a function of time, strain, and frequency. The rheometric dynamic analyzer (Rheometric Scientific, NJ, USA) was used in conjunction with 25-mm parallel disk fixtures.

The samples were heated in the rheometer for a period of 5 min before testing to allow the material to melt. The gap was set at 1 mm. Thus, the procedure of sample loading was standardized. The properties measured were the storage modulus ($G'$), loss modulus ($G''$), and complex viscosity ($\eta^*$). Before the frequency sweep, strain sweeps were performed at 190°C and 5 rad/s for each sample to determine the limits of the linear viscoelastic regime. The idea behind this analysis was to avoid the application of large strains that could stimulate the alignment of the clay particles.[30] In the following frequency sweep experiments, the strain was set to 10% to ensure that the experiments were carried out in the linear viscoelastic region, and the experiments were performed between the frequency range of 0.1 to 100 rad/s. To ensure good reproducibility of the results, each rheological measurement was replicated at least three times and reported at a 95% confidence interval.

## RESULTS AND DISCUSSION

### X-ray analysis of the organoclays

Figure 1 shows the XRD diffraction patterns of the organoclays and PB, showing that the interlayer distance of PB was 1.2 nm ($2\theta = 7.36°$). X-ray analysis showed that the *d*-spacing of PB increased from 1.2 to 2.64, 2.24, and 2.71 nm after the modifications with DMDA, TBHP, and TKA, respectively. These increases confirmed the intercalation of alkyl chains of the modifiers through the clay layers. The occurrence of ion exchange between the $Na^+$ ions of the clay and alkyl chains of the modifier could also be seen from the chemical analysis given in Table I, which shows the percentage decrease of $Na^+$ after modification with DMDA. This reduction implied that the exchangeable $Na^+$ ions of clays were mostly replaced by DMDA.

### XRD of the binary nanocomposites

Figure 2 shows the XRD patterns of organoclays and their binary composites with LOT. The compatibility between the LOT and clay was important because the clay could not be easily dispersed within the nonpolar LLDPE matrix without the help of a compatibilizer. Recently published data show that the use of LOT significantly increases the level of intercalation and exfoliation in LDPE-based nanocomposites.[31] The DMDA organoclay had a peak at $2\theta = 3.34°$, which corresponded to a *d*-spacing of 2.64 nm, and it was shifted to $2\theta = 2.35°$, which corresponded to a *d*-spacing of 3.75 nm upon compounding [Fig. 2(a)]. The results show that the *d*-spacing of DMDA increased in the LOT matrix, and the chains of LOT were intercalated between the clay galleries. This revealed that DMDA was compatible with LOT. The same conclusion could be observed from the XRD analysis of the TBHP organoclay [Fig. 2(b)]. Although the TBHP organoclay had a peak at $2\theta = 3.94°$, which corresponded to a *d*-spacing of 2.24 nm, its composite with LOT had a peak at $2\theta = 2.72°$, which corresponded to a *d*-spacing of 2.71 nm. The increase in the *d*-spacing of the organoclays upon compounding with LOT was 67% for DMDA, whereas it was 21% for TBHP. The TKA organoclay [Fig. 2(c)] had a peak at $2\theta = 3.26°$ ($d = 2.72$ nm), whereas the composite made with TKA had a peak at $2\theta = 3.73°$ ($d = 2.37$ nm); this indicated that the location of the clay peak was shifted to a smaller *d*-spacing upon melt compounding. This result shows that the TKA organoclay was not compatible with LOT, and it could not be intercalated or exfoliated in LOT. The bulky environment in TKA with long aliphatic tails (40 C) may have limited and sheltered the diffusion and access of LOT chains through the silicate layers.[32] Thus, TKA was not used further in the preparation of the ternary nanocomposites.

### XRD and TEM analysis of the ternary nanocomposites

Figure 3 shows XRD patterns of the pure DMDA organoclay and the ternary nanocomposites LLDPE/DMDA2/LOT5 and LLDPE/DMDA5/LOT12.5. The XRD patterns of the ternary nanocomposites showed that the characteristic peak of the organoclay shifted to smaller angles; this indicated that the polymer chains were intercalated between the clay galleries

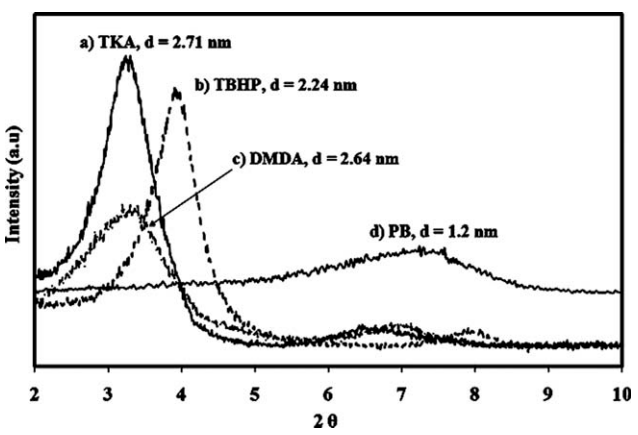


**Figure 1** XRD results of the modified clays: (a) TKA, (b) TBHP, (c) DMDA, and (d) PB.

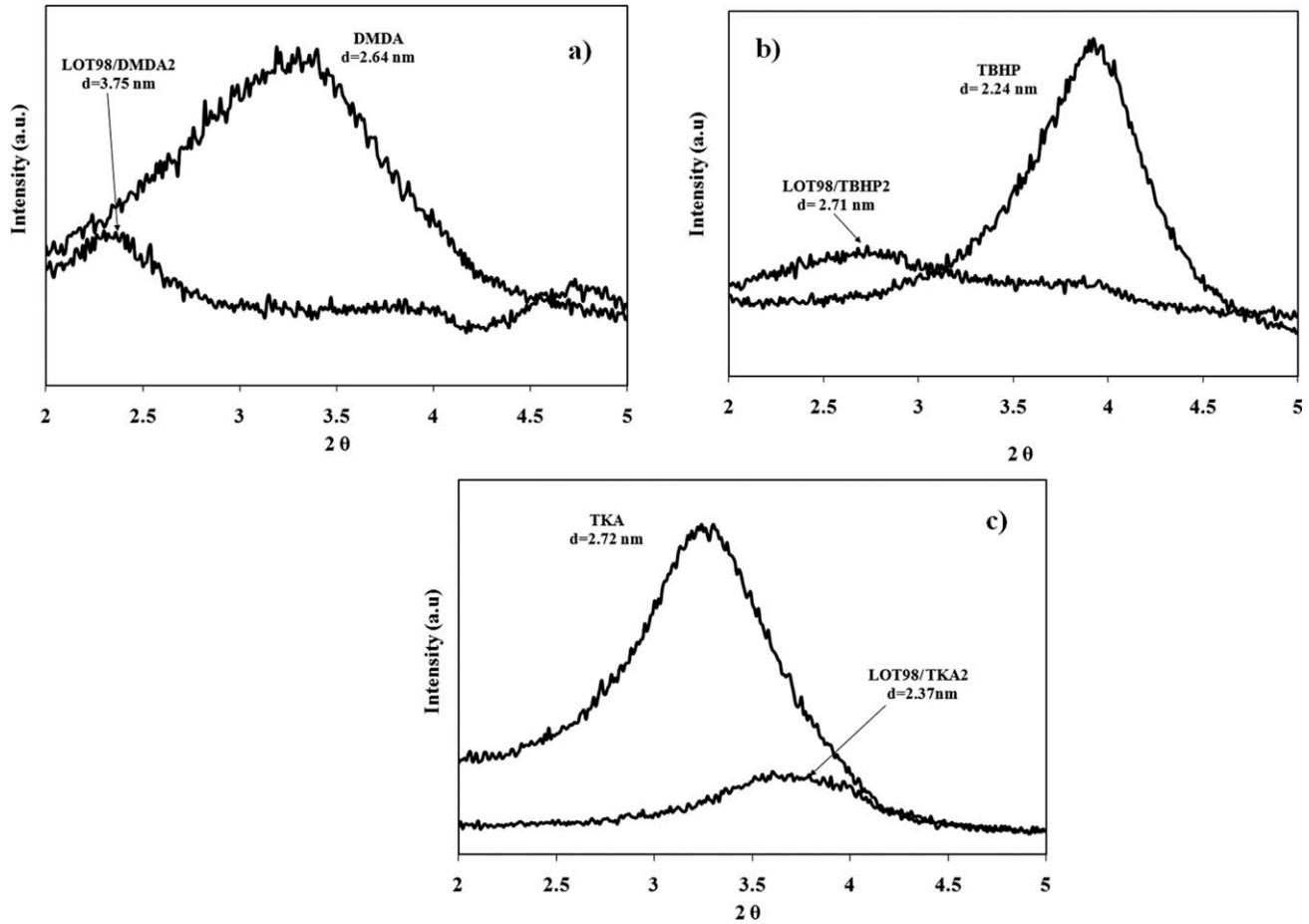


**Figure 2** XRD patterns of the organoclays and binary composites of LOT/organoclay with (a) DMDA, (b) TBHP, and (c) TKA.

in both sets of ternary nanocomposites. The location of the clay peak in the ternary nanocomposites with DMDA increased slightly from 3.39 to 3.67 nm as the clay concentration increased from 2 to 5%. This result was attributed to the fact that the compatibilizer/clay weight ratio was kept constant in both sets of ternary nanocomposites. TEM analysis of the LLDPE nanocomposite sample having 2% DMDA exhibited intercalated regions and exfoliated clay layers through the matrix (Fig. 4).

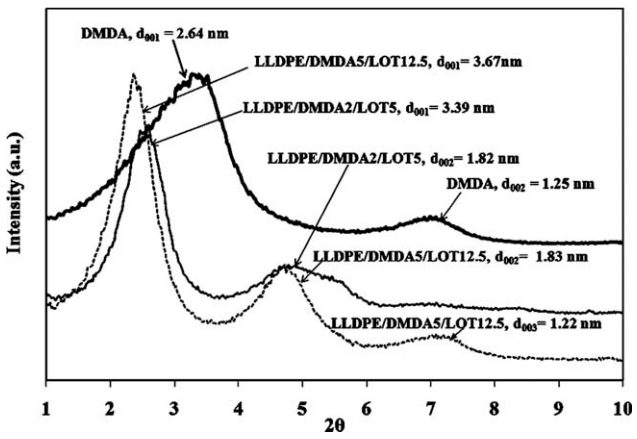


**Figure 3** XRD results of the DMDA clay and its ternary LLDPE/DMDA/LOT nanocomposites.

Although XRD is an extensively used technique in PCNs, it is a problematical issue in the literature to decide the degree of the distribution of the silicate layers or any structural nonhomogeneity in nanocomposites by XRD alone.[33] Morgan and Gilman[34] explained the inadequacy of XRD alone to characterize the state of dispersion of the clay layers and stated that XRD should be used in conjunction with TEM. It was stated that the absence of a peak may be misconceived. Depending on the problems due to sampling, orientation and poor calibration of most XRD instruments at very low angles, XRD diffractograms can yield wrong conclusions for intercalated and immiscible PCNs. Other authors also accepted the inadequacy of the data provided by the XRD alone[3,35–37] and used other techniques, such as TEM or rheology, to observe the state of dispersion of the clay layers. The situation was similar for the composite with TBHP that we used in this study. Figure 5 shows the XRD patterns of pure TBHP organoclay and the ternary nanocomposites LLDPE/TBHP2/LOT5 and LLDPE/TBHP5/LOT12.5. The XRD peaks

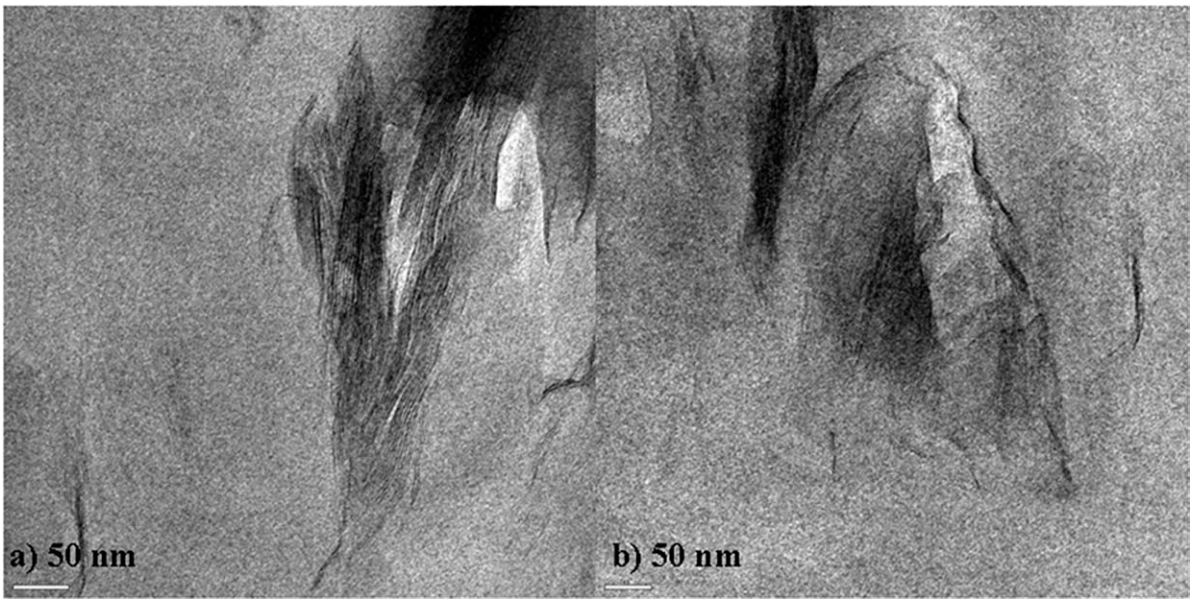


**Figure 4** TEM micrograph of LLDPE/DMDA2/LOT5.

corresponding to TBHP clay and to nanocomposites were seen at the same 2θ; this implied that the *d*-spacing of TBHP clay did not change upon compounding. However, TEM of LLDPE/TBHP2/LOT5 (Fig. 6) showed a mixed clay structure with intercalated regions together with some exfoliated single layers. These exfoliated regions significantly affected the rheological and mechanical properties of the nanocomposites, as discussed later.

### Rheological characterization

Figure 7 shows that addition of LOT to LLDPE did not have much effect on the viscoelastic behavior, especially in $G'$ and $G''$ of the LLDPE, thus the differences in the rheological parameters of compatibilized composites could be attributed to the presence of clay. LOT had little effect on $G''$, and it increased $G'$ slightly in the low-frequency region. Although $G'$ increased at low frequencies, the characteristic shoulder encountered in immiscible blends was not observed.[38] Because a small amount of LOT (5 wt %) was added to the LLDPE, a marginal decrease in η* of LLDPE was observed at high frequencies. This result, together with the fact that the $G'$ and $G''$ behaviors of the LLDPE/LOT blend were similar to those of LLDPE, implied that there was no liquid–liquid separation between LLDPE and LOT.[38]

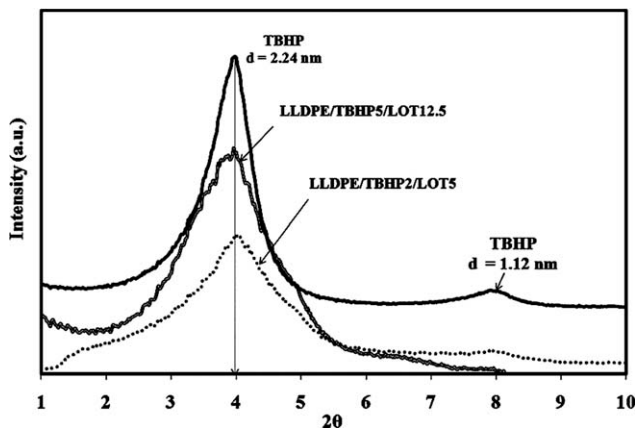


**Figure 5** XRD results of TBHP clay and its ternary LLDPE/TBHP/LOT nanocomposites.

Figure 8 shows the $G'/G'_m$ and $\eta^*/\eta^*_m$ values of the nanocomposites prepared with the DMDA organoclay at different clay contents, where $G'_m$ is the storage modulus of the base LLDPE and $G'$ is the storage modulus of the nanocomposite at the same frequency. $\eta^*_m$ in Figure 8 refers to complex viscosity of the base LLDPE and η* refers to the complex viscosity of the nanocomposite at the same frequency. Analogous figures obtained for the nanocomposites prepared with TBHP are given in Figure 9. Sample with 5 wt % DMDA organoclay showed higher $G'/G'_m$ and $\eta^*/\eta^*_m$ values compared to LLDPE, LLDPE/LOT, and the composite prepared with 2% DMDA. The nanocomposite of DMDA with low clay content showed Newtonian behavior similar to pristine LLDPE. The large surface area of clay particles produced colloidal interactions that enhanced $G'$ [Fig. 8(a)] at a clay content of 5%, especially in the low-frequency region.[39] At low frequencies, $G'$ was broadly separated, whereas the data gathered in the high-frequency region approached those of LLDPE and the LLDPE/LOT blend.

A minimum amount of exfoliated clay layers are needed to cause a significant increase in $G'$ of molten plastics.[30] This solidlike behavior formation is

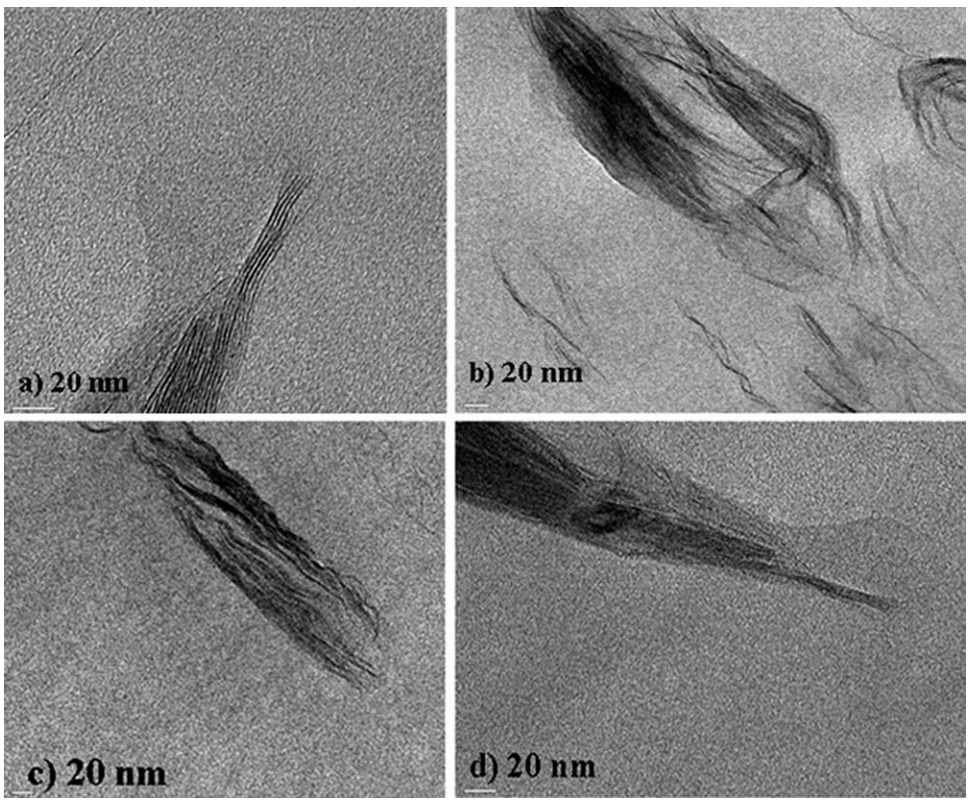


**Figure 6** TEM micrograph of LLDPE/TBHP2/LOT5.

attributed to the percolation network superstructure formation due to the exfoliated layers or stacks of intercalated layers, as reported by other researchers.[19,23,24,30] Galgali et al.[23] attributed typical rheological response, that is, solidlike behavior, of the clay–polymer nanocomposites to the frictional interactions between the silicate layers and not to the immobilization of confined polymer chains between the silicate layers. In other words, the solidlike behavior is due to the filler–filler interaction. The degree of this interaction depends on the level of exfoliation and intercalation of the organoclay; the higher the level of intercalation and exfoliation is, the higher the interaction is. The large anisotropy of the tactoids, specific surface area, and individual layers prevent the free rotation of these elements and is the main cause of the relatively low value of the percolation threshold compared to traditional composites.[22,30]

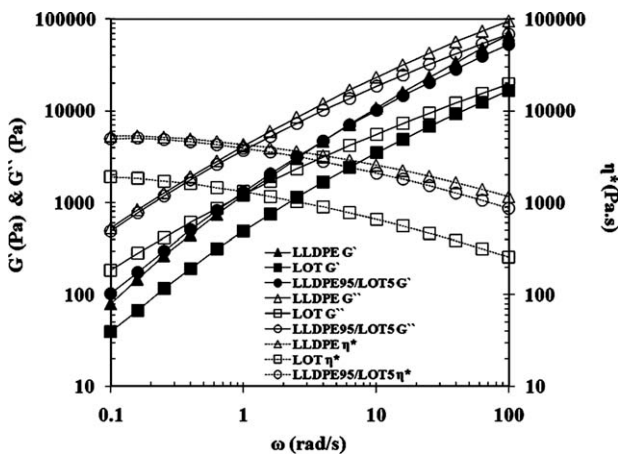


**Figure 7** Frequency dependence of $G'$, $G''$, and $\eta^*$ of LLDPE, LOT, and their LLDPE95/LOT5 blend.

Figure 9 indicates a slight increase in $G'/G'_m$ and $\eta^*/\eta^*_m$ at low frequencies with the TBHP organoclay at a clay content of 2%, whereas these ratios increased even more as the organoclay content increased to 5%. Enhancements in $G'$ in the low-frequency region and at high clay content were attributed to strong filler–polymer interactions, clay–matrix tethering, uniform nanoscale dispersion, and the much larger surface area of clay particles exposed to polymer chains.[40] A slight transition from liquidlike to pseudo-solidlike behavior could be observed for the nanocomposites with 2% TBHP in the low-frequency region, but this transition was more visible at 5% clay content. The term *solidlike* is related to the behavior of an elastic solid, whose $G'$ is independent of frequency, whereas *pseudo* means that the low-frequency plateau may be damaged by severe preloading.[41]

The chemistry of the salts used in clay modification affect the linear viscoelastic properties of PCNs. These effects could be attributed to changes in mesoscopic clay structure, short–long range clay ordering,

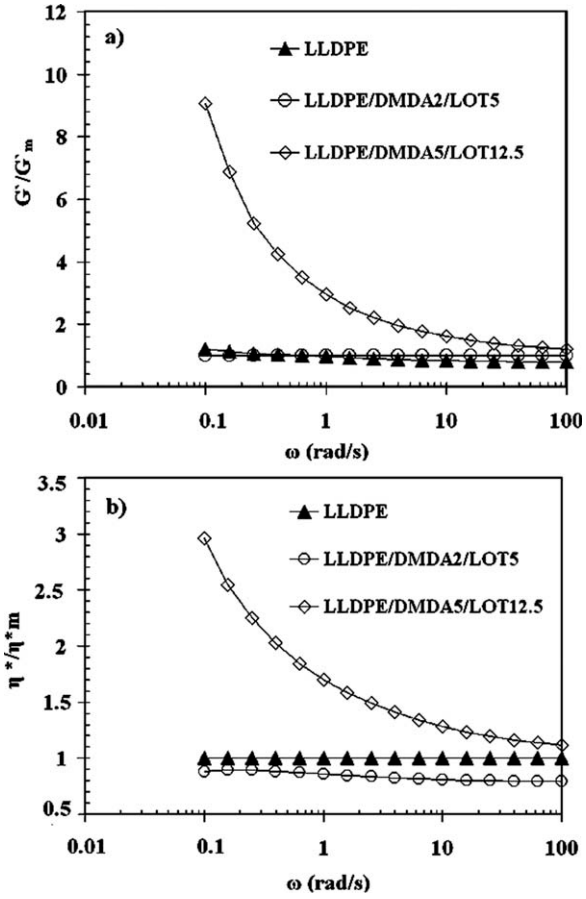


**Figure 8** Frequency (ω) dependence of $G'(\omega)/G'_m(\omega)$ and $\eta^*/\eta^*_m$ of the nanocomposites with DMDA organoclay.

or surface interactions between the clay and the polymer matrix.[21] Thus, it is important to study the effects of organoclay chemistry on the rheology of PCNs and to consider such interactions and structures. Figure 10 shows the frequency dependence of $G'/G'_m$ and $\eta^*/\eta^*_m$ of the samples prepared with different organoclays at a clay content of 2%. These figures indicate that the type of organoclay definitely had an effect on the rheological response of the composites. The degree of dispersion and the confinement of alkyl structures through the silicate layers affected the rheological properties. The effect of TBHP in the low-frequency region was more pronounced compared to DMDA (Fig. 10) at a clay content of 2 wt % and revealed strong interfacial interactions between the clay layers and the matrix for TBHP. TEM analysis also confirmed that TBHP had a higher degree of exfoliation compared to DMDA.

Figure 11 shows the comparison of the frequency dependence of rheological functions in nanocomposites prepared with 5 wt % organoclay. Again, in composites with TBHP, higher enhancements in $G'$ and $\eta^*$ are observed. Composites prepared with DMDA showed enhancement in $G'/G'_m$, not as high as those of TBHP but still higher compared to LLDPE; this implied an intercalated structure as well. Although XRD analysis is not highly sensitive to the differences in chemistry, $G'$ is a strong function of the chemistry, as depicted from Figure 11. Solomon et al.[21] explained this difference by two arguments. Surfactants adsorbed by the exterior surface of the area of the tactoids may intercede the differences in the attractive interparticle interactions that cause an increase in the hybrid network. In addition, the size and shape of the multiplatelet domains may depend on the surfactant chemistry. These delicate changes in the mesoscopic structure are poorly characterized by XRD, yet they can yield substantial rheological effects.

### Tensile properties of the nanocomposites

Representative stress–strain curves of LLDPE, binary blends of LOT and LLDPE, and ternary composites of LLDPE, organoclay, and LOT are shown in Figure 12. Figures 13–15 show the tensile strength, Young's modulus, and elongation at break, respectively, of the prepared materials. Analysis of the LOT+LLDPE blends indicated that the addition of 12.5 wt % LOT to LLDPE did not increase the tensile strength of LLDPE, but it increased the Young's modulus of LLDPE by 8%. The

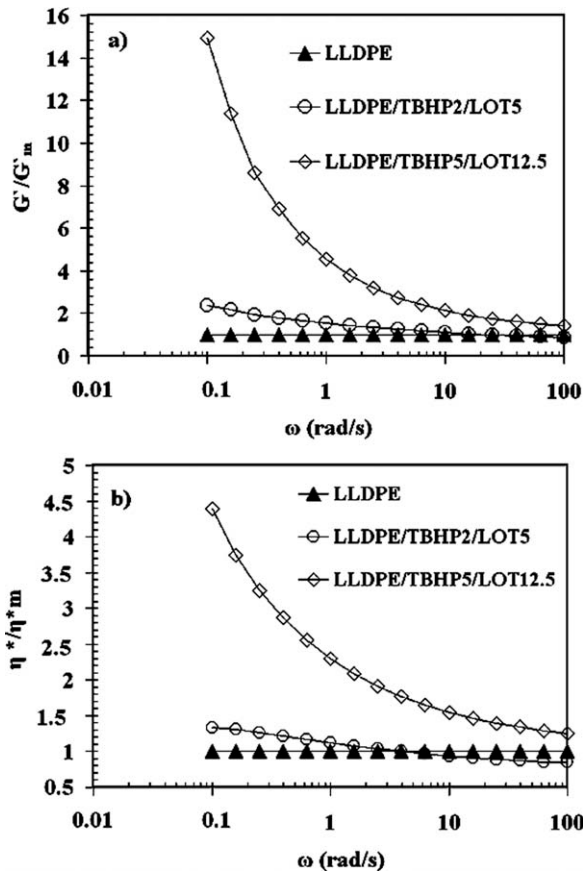


**Figure 9** Frequency (ω) dependence of $G'(\omega)/G'_m(\omega)$ and $\eta^*/\eta^*_m$ of the nanocomposites with TBHP organoclay.

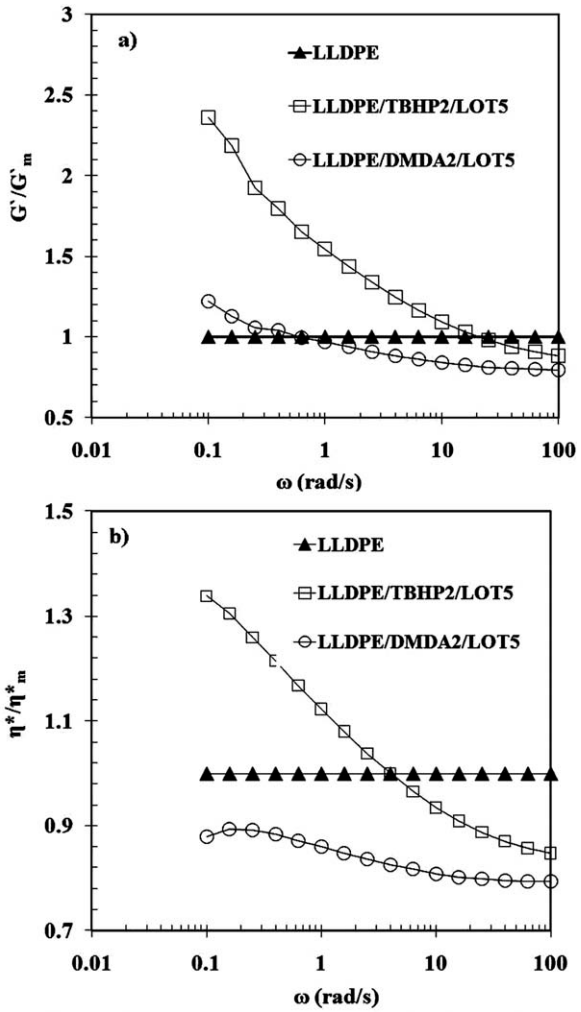


**Figure 10** Frequency (ω) dependence of $G'(\omega)/G'_m(\omega)$ and $\eta^*/\eta^*_m$ of the nanocomposites with 2% DMDA and TBHP organoclay.

addition of 5 wt % elastomer LOT to LLDPE increased the Young's modulus of LLDPE by 13% and the tensile strength of LLDPE by 5%, but these properties decreased as the LOT content was increased to 12.5 wt %. Hotta and Paul[17] found similar trends in LLDPE and MA-grafted polyethylene (LLDPE-*g*-MA) blends. In their study, 5, 8.5, and 16.5 wt % additions of LLDPE-*g*-MA to LLDPE increased the strength and Young's modulus, whereas 33 wt % addition of LLDPE-*g*-MA decreased the Young's modulus from 190 to 168 MPa. Decreases in the modulus and tensile strength at high LOT contents were attributed to the dilution effect of LOT because LOT has a lower tensile strength compared to LLDPE.[42]

Analysis of the ternary nanocomposites indicated that the addition of clay to LLDPE/LOT not only increased the strength and modulus of LLDPE/LOT but also considerably increased the elongation at break.

Young's moduli of the ternary nanocomposites prepared with TBHP at two clay contents were higher than those of the nanocomposites with

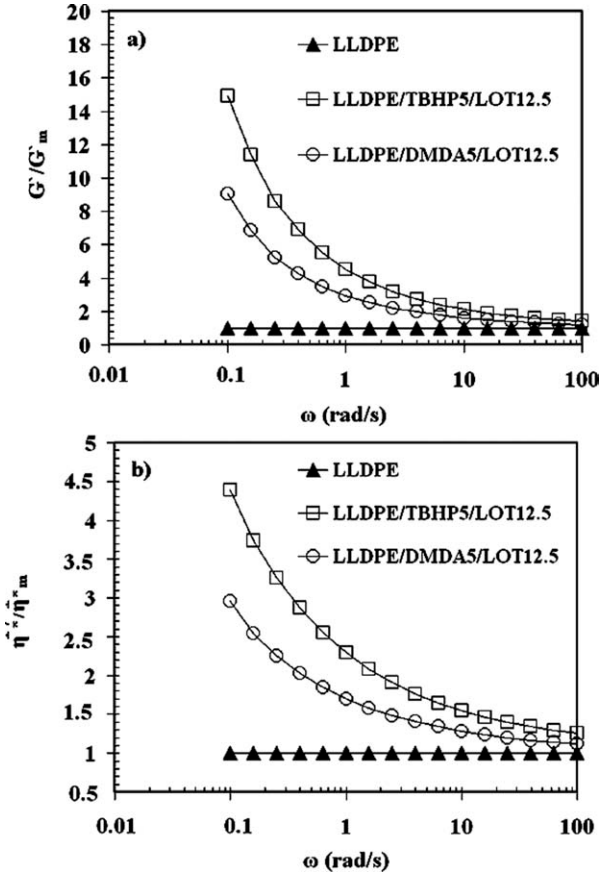


**Figure 11** Frequency (ω) dependence of $G'(\omega)/G'_m(\omega)$ and $\eta^*/\eta^*_m$ of the nanocomposites with 5% DMDA and TBHP organoclay.

DMDA (Fig. 14). The error band for the nanocomposite with TBHP was very large, and the findings held within the error range. Although DMDA showed a high extent of intercalation, that is, a high *d*-spacing in the XRD measurement, TEM and rheological analysis showed that it was less compatible with LLDPE compared to TBHP. This behavior was also seen in the modulus results because enhancement with DMDA was lower than that with TBHP. This may have been due to the smaller degree of

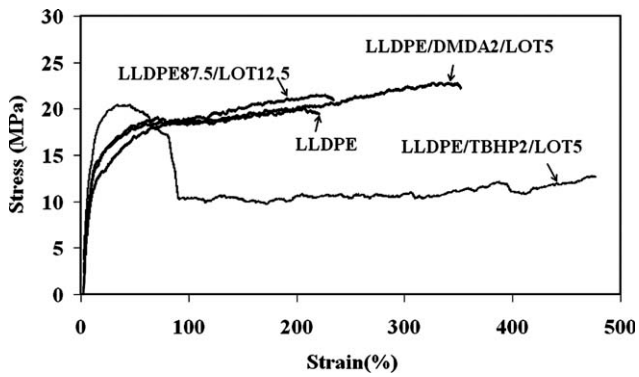


**Figure 12** Stress–strain diagram of the LLDPE composites.

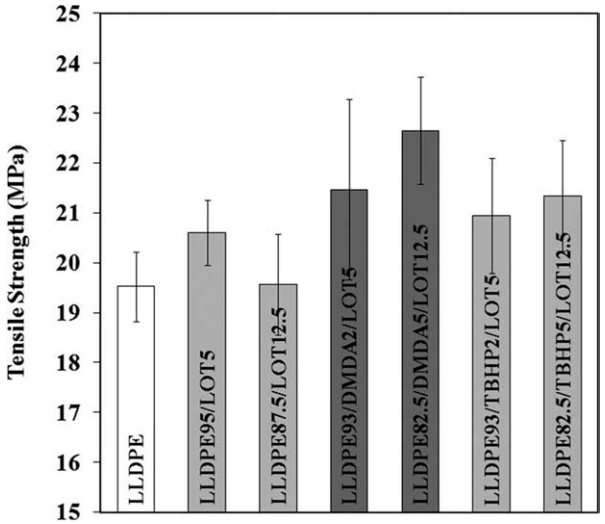


**Figure 13** Tensile strength of the LLDPE composites.

exfoliation with DMDA, which may have resulted in low interaction between the filler and the matrix. TEM micrograph of the sample with TBHP indicated a higher degree of exfoliation compared to DMDA. Hotta and Paul[17] studied LLDPE/organoclay/LLDPE-*g*-MA nanocomposites and found that the LLDPE matrix with low polarity had a higher affinity to organoclays with two alkyl tails than the ones with one alkyl tail, and maximizing the alkyl tails led to better dispersion in this polymer. The present situation is somewhat similar. DMDA had two long alkyl tails with 18 C atoms in each and two methyl groups. TBHP had one long alkyl tail with 16 C atoms and three tails with 4 C atoms. In other words, TBHP had a higher number of effective tails in comparison to DMDA. Thus, the ternary nanocomposites with TBHP exhibited a higher level of exfoliation, as observed from TEM, and a higher Young's modulus in comparison to its counterparts with DMDA.

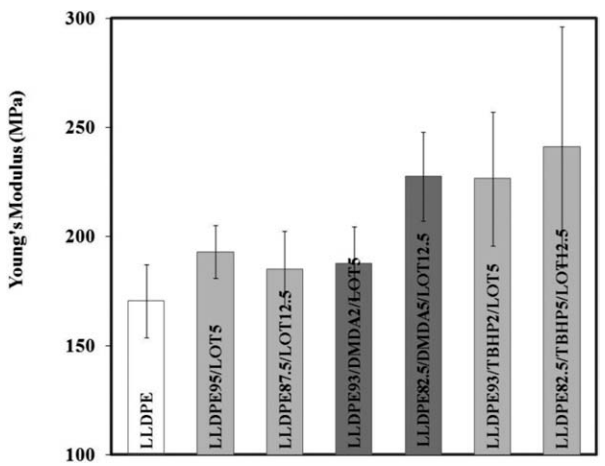


**Figure 14** Young's modulus of the LLDPE composites.

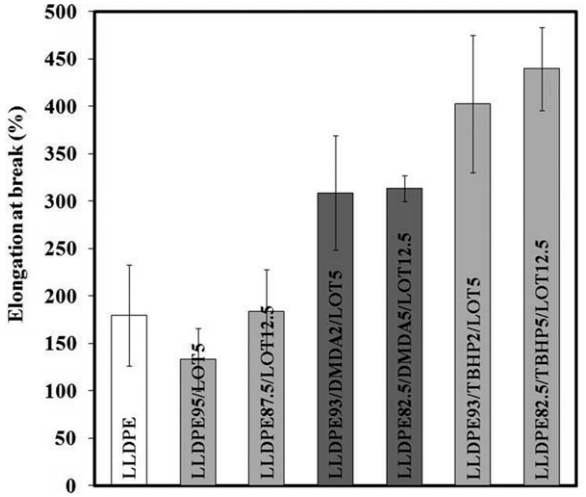


**Figure 15** Elongation at break of the LLDPE composites.

Figure 15 shows the elongation at break of the nanocomposites. An increase in strength due to decreased ductility is known to occur by the incorporation of clay because inorganic particles cannot be strained by external stresses but behave as stress concentrators during the extension process.[5] The relation between the elongation at break and the tensile strength of the samples mentioned previously was confirmed in the case of TBHP clay, in which its composites showed a higher elongation at break but lower strength compared to composites of DMDA. In the case of DMDA, and especially in TBHP, the elongation at break values were much higher than those of the neat LLDPE and showed enhancement in the ability of the material to absorb energy because of good adhesion between the filler and the matrix. This increase in the elongation at break of the nanocomposites is in contrast with most of the published literature because the addition of organoclay generally increases the strength of the neat polymer but decreases its ductility.[17,43] However, the results of Zhang and Sundararaj[38] were similar to the results of this study, as they observed an increase in the ductility of LLDPE/maleic anhydride grafted polyethylene (PEMA)/organoclay composites. In the ternary composites of the present study, the organoclays DMDA and TBHP acted as crack stoppers, and the composites could elongate to a high extent. Also, the strain at break of pure LOT was 600%, as given by the manufacturer. This value was much higher than the strain at break of the LLDPE used here (180%); thus, the addition of LOT also increased the strain at break of the ternary nanocomposites. The area under the stress–strain curves could be taken as a measure for the energy that was dissipated by plastic deformation within the sample; thus, the results in Figure 15 imply that the TBHP nanocomposites were superior to the DMDA nanocomposites in terms of ductility.

## CONCLUSIONS

Organoclays produced with different quaternary alkyl surfactants were used in the production of ternary nanocomposites of LLDPE/organoclay/LOT and binary composites of LOT/organoclay in a batch mixer. XRD and TEM analysis showed partially intercalated and exfoliated regions in the ternary nanocomposites prepared with the organoclays DMDA and TBHP. TKA, with a crowded C environment (40 C), could not intercalate when it was compounded with the compatibilizer LOT because these long alkyl tails limited the diffusion of LOT chains through clay layers. Rheological characterization was used to assess the degree of dispersion in the nanocomposites as a complementary tool to XRD, TEM, and mechanical characterization. Rheological analysis revealed that in the low-frequency region, the nanocomposite prepared with TBHP organoclay displayed increase in $G'$ (1393% with respect to LLDPE) and $\eta^*$ (339% with respect to LLDPE). The nanocomposite prepared with DMDA organoclay displayed a lower increase in $G'$ (807% with respect to LLDPE) and $\eta^*$ (196% with respect to LLDPE). An increase in the organoclay content increased both of these rheological properties. TEM analysis of the ternary composite LLDPE/TBHP2/LOT5 showed that intercalated and exfoliated single layers were present in this material in accordance with the rheological property enhancement with this organoclay. The tensile strength and Young's modulus values of the samples prepared with TBHP and DMDA were higher compared to those of neat LLDPE. The ductility of LLDPE and LLDPE/LOT increased through the addition of the organoclays TBHP and DMDA.

The authors thank Prof. Dr. D. M. Kalyon and Dr. H. Gevgilili (Highly Filled Materials Institute, Stevens Institute of Technology) for scientific contributions and the use of their facilities.

## References

1. Usuki, A.; Kawasumi, M.; Kojima, Y.; Okada, A.; Kurauchi, T.; Kamigaito, O. J. Mater Res 1993, 8, 1174.
2. Quintanilla, L. M. L.; Valdes, S. S.; Valle, L. F. R.; Rodriguez, F. J. M. J Appl Polym Sci 2006, 100, 4748.
3. Lee, J. W.; Kim, M. H.; Choi, W. M.; Park, O. O. J Appl Polym Sci 2006, 99, 1752.
4. Chow, W. S.; Mohd, I. Z. A.; Karger-Kocsis, J.; Apostolov, A. A.; Ishiaku, U. S. Polymer 2003, 44, 7427.
5. Contreras, V.; Cafiero, M.; Silva, S. D.; Rosales, C.; Perera, R.; Matos, M. Polym Eng Sci 2006, 46, 1111.
6. Jin, D. W.; Seol, S. M.; Kim, G. H. J Appl Polym Sci 2009, 114, 25.
7. Stoeffler, K.; Lafleur, P. G.; Denault, J Polym Eng Sci 2008, 48, 1449.
8. Qin, H.; Zhang, S.; Zhao, C.; Hu, G.; Yang, M. Polymer 2005, 46, 8386.
9. Osman, M. A.; Mittal, V. Macromol Rapid Commun 2004, 25, 1145.
10. Osman, M. A.; Mittal, V.; Suter, U. W. Macromol Chem Phys 2007, 208, 68.
11. Smart, G.; Kandola, B. K.; Horrocks, A. R.; Nazare, S.; Marney, D. Polym Adv Tech 2008, 19, 658.
12. Chen, B.; Evans, J. G. Polym Int 2005, 54, 807.
13. Calderon, J. U.; Lennox, B.; Kamal, M. R. Appl Clay Sci 2008, 40, 90.
14. Hedley, C. B.; Yuan, G.; Theng, B. K. G. Appl Clay Sci 2007, 35, 180.
15. Kozak, M.; Domka, L. J. Phys Chem Solid 2004, 65, 441.
16. Lee, J. Y.; Lee, H. K. Mater Chem Phys 2004, 85, 410.
17. Hotta, S.; Paul, D. R. Polymer 2004, 45, 7639.
18. Kawasumi, M.; Hasegawa, N.; Kato, M.; Usuki, A.; Okada, A. Macromolecules 1997, 30, 6333.
19. Wu, D.; Zhou, C.; Fan, X.; Mao, D.; Bian, Z. Polym Degrad Stab 2005, 87, 511.
20. Prasad, R.; Gupta, R. K.; Cser, F.; Bhattacharya, S. N. J Appl Polym Sci 2006, 101, 2127.
21. Solomon, M. J.; Almusallam, A. S.; Kurt, F. Macromolecules 2001, 34, 1864.
22. Li, J.; Zhou, C.; Wang, G.; Zhao, D. J Appl Polym Sci 2003, 89, 3609.
23. Galgali, G.; Ramesh, C.; Ashish, L. Macromolecules 2001, 34, 852.
24. Durmus, A.; Kasgoz, A.; Macosko, C. W. J Macromol Sci Part B: Phys 2008, 47, 608.
25. Demirkol, E.; Kalyon, D. M. J Appl Polym Sci 2003, 104, 1391.
26. Nikkhah, S. J.; Ramazani, S. A. A.; Baniasadi, H.; Tavakolzadeh, F. Mater Des 2009, 30, 2309.
27. Ramazani, S. A. A.; Tavakolzadeh, F.; Baniasadi, H. Polym Compos 2009, 30, 1388.
28. Ramazani, S. A. A.; Tavakolzadeh, F. Macromol Symp 2008, 274, 65.
29. Seyidoglu, T. Ph.D. Thesis, Middle East Technical University, 2010.
30. Rohlmann, C.; Failla, M. D.; Quinzani, L. M. Polymer 2006, 47, 7795.
31. Coskunses, F.; Yilmazer, U. J Appl Polym Sci 2011, 120, 3087.
32. Kadar, F.; Szazdi, L.; Fekete, E.; Pukanszky, B. Langmuir 2006, 22, 7848.
33. Vaia, R. A.; Jandt, K. D.; Edward, J. K.; Giannelis, E. P. Chem Mater 1994, 6, 1017.
34. Morgan, A. B.; Gilman, J. W. J Appl Polym Sci 2003, 87, 1329.
35. Lertwimolnun, W.; Vergnes, B. Polym Eng Sci 2006, 46, 314.
36. Liu, H.; Lim, H. T.; Ahn, K. H.; Lee, S. J. J Appl Polym Sci 2007, 104, 4024.
37. Eckel, D. F.; Balogh, M. P.; Fasulo, P. D.; Rodgers, W. R. J Appl Polym Sci 2004, 93, 1110.
38. Zhang, M.; Sundararaj, U. Macromol Mater Eng 2006, 291, 697.
39. Rohlmann, C. O.; Horst, M. F.; Quinzani, L. M.; Failla, M. D. Eur Polym J 2008, 44, 2749.
40. Barick, A. K.; Tripathy, D. K. Polym Eng Sci 2010, 50, 484.
41. Drozdov, A. D.; Jensen, E. A.; Christiansen, J. C. Int J Nanotech Appl 2008, 2, 1.
42. Isik, I.; Yilmazer, U.; Bayram, G. Polym Compos 2008, 29, 133.
43. Fornes, T. D.; Yoon, P. J.; Hunter, D. L.; Keskkula, H.; Paul, D. R. Polymer 2001, 42, 9929.